Pyrrolidinium-Based Ionic Liquids. 1-Butyl-1-methyl Pyrrolidinium Dicyanoamide: Thermochemical Measurement, Mass Spectrometry, and ab Initio Calculations

Vladimir N. Emel'yanenko,[†] Sergey P. Verevkin,*[,†] Andreas Heintz,*[,†] Jo-Anne Corfield,[‡] Alexey Deyko,[‡] Kevin R. J. Lovelock,[‡] Peter Licence,[‡] and Robert G. Jones*[,‡]

Department of Physical Chemistry, University of Rostock, Hermannstrasse 14, 18051 Rostock, Germany, and Department of Physical Chemistry, School of Chemistry, University Park, University of Nottingham, Nottingham, UK NG7 2RD

Received: April 15, 2008; Revised Manuscript Received: July 3, 2008

The standard molar enthalpy of formation of the ionic liquid 1-butyl-1-methylpyrrolidinium dicyanamide has been determined at 298 K by means of combustion calorimetry, while the enthalpy of vaporization and the mass spectrum of the vapor (ion pairs) have been determined by temperature-programmed desorption and line of sight mass spectrometry. Ab initio calculations for 1-butyl-1-methylpyrrolidinium dicyanamide have been performed using the G3MP2 and CBS-QB3 theory, and the results from homodesmic reactions are in excellent agreement with the experiments.

Introduction

Room temperature ionic liquids (ILs), which are entirely composed of ions, are currently attracting considerable attention as potentially benign solvents for many areas such as fuel cells, rechargeable batteries, and "green solvents".[1] Pyrrolidinium-based ionic liquids with the dicyanamide anion are hygroscopic and completely miscible with water. The dicyanamide ionic liquids are also soluble in most laboratory solvents (exceptions are hexane, toluene, and low boiling petroleum).[2] Thus, these new water-miscible ionic liquids of relatively low viscosity have a considerable potential as a reaction medium.[3] Here we report the first experimental determination of the gaseous enthalpy of formation, $\Delta_f H^\circ_m(g)$, and enthalpy of vaporization, $\Delta^g_l H_m$, of an ionic liquid of this type, namely: 1-butyl-1-methylpyrrolidinium dicyanamide [$Pyrr_{14}$][dca] (see Figure 1). We also report a systematic study of the thermochemical properties of [$Pyrr_{14}$][dca] according to the general equation:

$$\Delta_f H^\circ_m(g) = \Delta_f H^\circ_m(l) + \Delta^g_l H_m \qquad (1)$$

where the standard molar enthalpy of formation of liquid phase [$Pyrr_{14}$][dca], $\Delta_f H^\circ_m(l)$, was obtained from the calorimetrically measured enthalpy of combustion and the molar enthalpy of vaporization, $\Delta^g_l H_m$, was obtained by temperature programmed desorption (TPD) using line of sight mass spectrometry (LOSMS). In addition, we also report the mass spectrum of the IL and its decomposition at elevated temperatures, and ab initio calculations of the cation, the anion, and the neutral ion pair of [$Pyrr_{14}$][dca] in the gaseous phase using the G3* compound methods. Our new results for the vaporization enthalpy, $\Delta^g_l H_m$, and for the enthalpy of formation, $\Delta_f H^\circ_m(g)$, of the [$Pyrr_{14}$][dca] can be used as reference values for molecular modeling studies and validation of the quality of ab initio caculations.

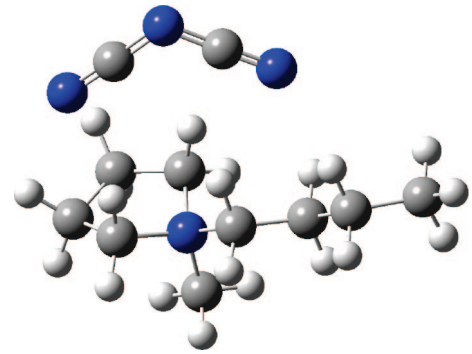

Figure 1. Stable conformation [$Pyrr_{14}$][dca] (G3MP2).

Experimental Section

Materials. The sample of 1-butyl-1-methylpyrrolidinium dicyanamide [$Pyrr_{14}$][dca], $[C_4H_8N(CH_3)C_4H_9]^+[N(CN)_2]^- = C_{11}H_{20}N_4$, CAS 370865-80-8 was of commercial origin (Merck product 4.90044). The sample contained <1000 ppm of halide and <10000 ppm of water according to specifications stated by the suppliers. This level of halide impurity did not impact the experiments. Prior to experiments in Rostock, the IL samples were subjected to vacuum evaporation at 333 K and 10^{-2} mbar for more than 24 h to reduce possible traces of solvents and moisture. The water concentration in [$Pyrr_{14}$][dca] of 727.2 ppm was determined by Karl Fischer titration shortly before each experiment and an appropriate correction applied to the results. We used Mettler DL35 Karl Fischer Titrator with Hydranal Composite 2, Hydranal Methanol Dry, and Hydranal Eichstandard 5.0 (Riedel-de Haen). Samples of the IL was kept and handled under nitrogen stream in a special glass device furnished with a septum for the sample extraction using a syringe. For the vaporization and mass spectrometry experiments in Nottingham the IL samples were degassed at 10^{-2} mbar and 343 K, followed by degassing in the ultrahigh vacuum chamber (UHV) at 10^{-9} mbar and 300 K.

* To whom correspondence concerning the combustion experiments and ab initio calculations should be addressed. (S.V.) E-mail: sergey.verevkin@uni-rostock.de. Fax:+49 381 498 6502. Tel: +49 381 498 6508. (A.H.) E-mail: andreas.heintz@uni-rostock.de. Fax: +49 381 498 6502. Tel: +49 381 498 6501. To whom correspondence concerning mass spectrometry and the enthalpy of vaporization should be addressed. (R.J.) E-mail: robert.g.jones@nottingham.ac.uk. Fax: +44 115 9513562. Tel: +44 115 9513468.

† University of Rostock.

‡ University of Nottingham.

10.1021/jp803238t CCC: $40.75
Published on Web 08/26/2008

TABLE 1: Formula, Density ρ (T = 293 K), Massic Heat Capacity c_p (T = 298.15 K), and Expansion Coefficients $(\delta V/\delta T)_p$ of the Materials Used in the Present Study

compound	formula	ρ, g·cm^{-3}	c_p,[b] J·K^{-1} g^{-1}	$10^{-6} \times (\delta V/\delta T)_p$,[c] dm^3·K^{-1}
[Pyrr$_{14}$][dca]	$C_{11}H_{20}N_4$	0.950[a]	1.20	1.0
polyethene[d]	$CH_{1.93}$	0.920	2.53	0.1
cotton[e]	$CH_{1.774}O_{0.887}$	1.500	1.67	0.1

[a] Merck catalogue. [b] Calculated using procedure suggested by Chickos and Acree.[21] [c] Estimated. [d] From 10 combustion experiments, $\Delta_c u^\circ = -(46361.0 \pm 4.0)$ J·g^{-1}. [e] From 10 combustion experiments, $\Delta_c u^\circ = -(16945.2 \pm 4.2)$ J·g^{-1}.

TABLE 2: Results for Typical Combustion Experiments at T = 298.15 K (p° = 0.1 MPa) of the [Pyrr$_{14}$][dca][a]

m (substance), g[b]	0.390513	0.391821	0.390204	0.407304	0.357867	0.294346
m' (cotton), g[b]	0.001088	0.001053	0.001094	0.000877	0.002888	0.002879
m'' (polyethene), g[b]	0.28828	0.271919	0.286455	0.3019	0.290723	0.279187
ΔT_c, K[c]	1.82356	1.77571	1.81679	1.90572	1.75723	1.57164
$(\epsilon_{calor}) \times (-\Delta T_c)$, J	−27001.7	−26293.2	−26901.3	−28218.2	−26011.6	−23264.3
$(\epsilon_{cont}) \times (-\Delta T_c)$, J	−33.83	−32.77	−33.69	−35.63	−32.52	−28.55
ΔU_{decomp} HNO_3, J	77.05	72.87	73.46	80.33	73.46	68.39
ΔU_{corr}, J[d]	9.34	8.07	8.3	8.75	7.95	6.92
$-m' \times \Delta_c u'$, J	18.44	17.84	18.54	14.86	48.94	48.78
$-m'' \times \Delta_c u''$, J	13364.95	12606.44	13280.34	13996.39	13478.21	12943.39
$\Delta_c u^\circ$ (liq), (J·g^{-1})	−34738.3	−34762.6	−34736.6	−34749.2	−34749	−34739.4

[a] For the definition of the symbols, see ref 7, macrocalorimeter: T_h = 298.15 K; V(bomb) = 0.2664 dm^3; p^i(gas) = 3.04 MPa; $m^i(H_2O)$ = 1.00 g. [b] Masses obtained from apparent masses. [c] $\Delta T_c = T^f - T^i + \Delta T_{corr}$; $(\epsilon_{cont}) \times (-\Delta T_c) = (\epsilon^i_{cont}) \times (T^i - 298.15\ K) + (\epsilon^f_{cont}) \times (298.15\ K - T^f + \Delta T_{corr.})$. [d] ΔU_{corr}, the correction to standard states, is the sum of items 81 to 85, 87 to 90, 93, and 94 in ref 7. [f] ϵ = 14807.1 ± 1.0 J·K^{-1} (for 1−4 experiments); ϵ = 14802.6 ± 0.9 J·K^{-1} (for 5−6 experiments).

TABLE 3: Thermochemical Data at T = 298.15 K (p° = 0.1 MPa) for [Pyrr$_{14}$][dca] (in kJ·mol^{-1})

$\Delta_c H_m^\circ$ (liq)	$\Delta_f H^\circ_m$(liq)	$\Delta_l{}^g H_{m\ exp}$	$\Delta_l{}^g H_{m\ calc}$	$\Delta_f H_m^\circ$ (g)
−7244.8 ± 2.3	57.9 ± 2.8	161.0 ± 2.0	—	218.9 ± 3.4
—	—	—	159.7[a]	217.6 G3MP2
			159.1[a]	217.0 CBS-QB3

[a] The differences between the $\Delta_f H^\circ_m$(g) derived using the ab initio methods and the $\Delta_f^\circ H$m(liq) from the combustion experiments.

Thermochemical Measurements. Combustion Calorimetry (Rostock). An isoperibol bomb calorimeter was used for the measurement of energy of combustion of [Pyrr$_{14}$][dca]. Six successful experiments were carried out for this compound (see Tables 1 and 2). The detailed procedure has been described previously.[4,5] The combustion products were examined for carbon monoxide (Dräger tube) and unburned carbon, but none was detected. The energy equivalent of the calorimeter ϵ_{calor} was determined with a standard reference sample of benzoic acid (sample SRM 39i, NIST). Correction for nitric acid formation was based on the titration with 0.1 mol·dm^{-3} NaOH (aq). The atomic weights used were those recommended by the IUPAC Commission.[6] The sample masses were reduced to vacuum, taking into consideration the density value ρ(293 K) = 0.95 g·cm^{-3} for the liquid [Pyrr$_{14}$][dca].[2] For converting the energy of the actual bomb process to that of the isothermal process, and reducing to standard states, the conventional procedure[7] was applied. Values of the standard specific energies of combustion $\Delta_c u^\circ$, together with the necessary auxiliary quantities, are given in Tables 1 and 2. To derive $\Delta_f H^\circ_m$(l) from $\Delta_c H^\circ_m$, molar enthalpies of formation of H_2O (l) and CO_2 (g) were taken, as assigned by CODATA.[8] Table 3 lists the derived standard molar enthalpy of combustion, and standard molar enthalpy of formation of the [Pyrr$_{14}$][dca]. The total uncertainty was calculated according to the guidelines presented by Olofsson.[9] The uncertainty assigned to $\Delta_f H^\circ_m$ is twice the overall standard deviation and includes the uncertainties from calibration, from the combustion energies of the auxiliary materials, and the uncertainties of the enthalpies of formation of the reaction products H_2O and CO_2.

Thermochemical Measurements. Transpiration Method (Rostock). Vapor pressures and enthalpy of vaporization, of several ILs such as [BMIM][dca] and [EMIM][NTf$_2$] have successfully been determined using the method of transference in a saturated stream of helium.[5] In short, the sample of the IL (approximately 0.5 g) is mixed with glass beads and placed in a thermostatted U-tube of length 10 cm and diameter 0.5 cm. A preheated helium stream is passed through the U-tube at constant temperature (±0.1 K). The flow rate of the helium stream is optimized in order to reach the saturation equilibrium of the transporting gas at each temperature under study. The material transported is condensed in a cold trap. The amount of condensed product in the trap is determined by weighing (±0.0001 g). In this work we tried to perform the transpiration experiments on [Pyrr$_{14}$][dca] in the temperature range 393 to 473 K at a flow rate of 8.5 dm^3·h^{-1}. Such a flow rate is close to the upper limit of our apparatus 12 dm^3·h^{-1}, where the saturation of the transporting gas with the IL in the saturation tube is still ensured. However, no condensate was detected in the cold trap. Observation of the sample in the saturation tube revealed an intense brown coloration of the IL after the heating. Clearly, neither the vapor pressure nor the enthalpy of vaporization of this IL can be determined using the transpiration method. Thus, another method, line of sight mass spectrometry,[10] has been applied for this purpose.

Thermochemical Measurements. Line of Sight Mass Spectrometry (Nottingham). The sample of [Pyrr$_{14}$][dca] was evaporated from a thin liquid film sample holder (dipstick) in UHV, the desorbed vapor being analyzed by LOSMS. The apparatus comprised a 6 mm wide dipstick made from silver (for good heat conduction), mounted on the end of a single

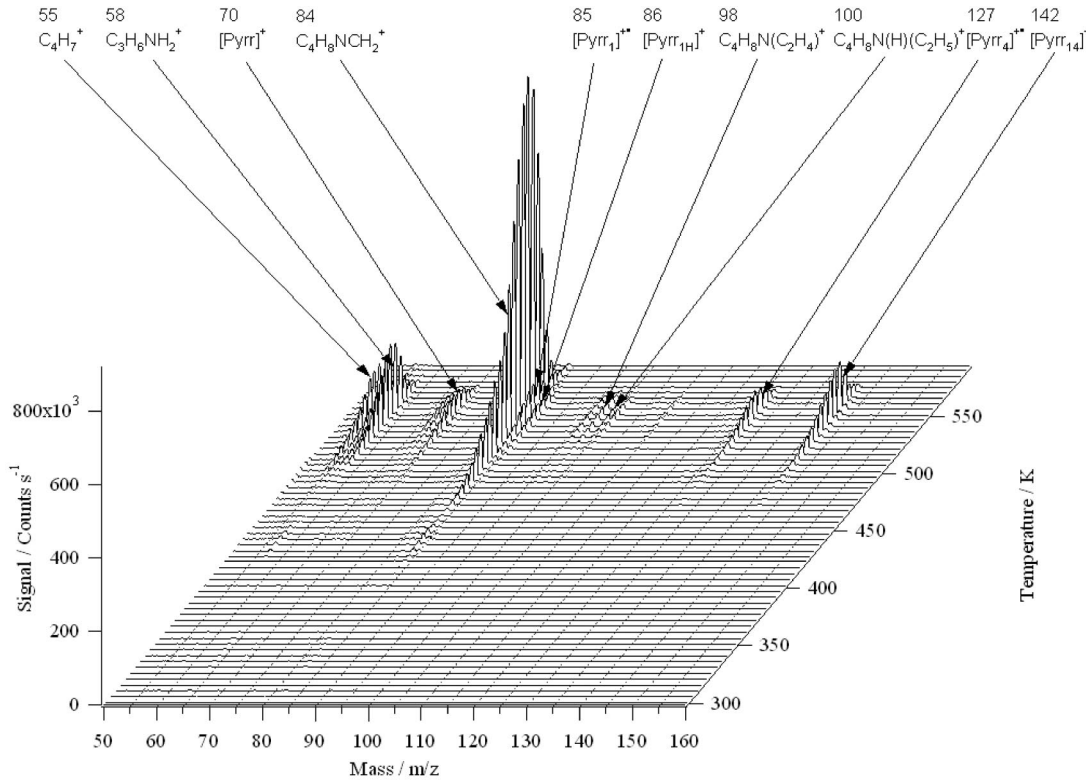

Figure 2. Multiple mass spectra of [$Pyrr_{14}$][dca] taken during temperature-programmed desorption.

crystal sample holder in an UHV chamber normally used for single crystal surface studies. The IL, in a 1 mL glass sample bottle, was inserted into a load lock and after pumping to $<10^{-7}$ mbar, was transferred to the UHV chamber (10^{-9} mbar) containing the dip-stick and LOSMS.

A thin film (typically 0.2 mm thick) of the IL adhering to the vertical surface of the dipstick was formed by immersion into the liquid (8 mm) followed by emersion. The thin film was then thermally evaporated and the vapor analyzed by LOSMS.[10] Several modes of operation were used. In a normal TPD run (300−550 K, 0.052 ± 0.002 K s^{-1}, temperature monitored using a type K thermocouple), the intensities of several ions from the vapor were monitored by LOSMS. Alternatively, during a TPD run, complete mass spectra could be measured every minute, to ensure all species in the vapor were recorded. The dip-stick temperature could also be ramped to a given value and then held constant while particular ions or complete mass spectra were measured. Finally, during desorption at constant temperature a flag could be moved into the line of sight vapor beam between the sample and the LOSMS, allowing us to differentiate between species which were in the beam (i.e., genuine IL vapor, contaminants and any decomposition products which originated from the IL sample itself) and those which originate from material deposited inside the mass spectrometer and then redesorbed or cracked by the heat/electrons within the mass spectrometer itself.

In LOSMS a pulse-counting mass spectrometer (Hiden RC511, mass range $m/z = 1-511$) is shrouded by a cryopump (liquid nitrogen, 80 K) having two apertures which establish a line of sight between the ionization volume of the mass spectrometer and a patch 7.5 mm in diameter at the sample (dipstick) surface.[10−13] Only species flying by line of sight from the sample, through both apertures, to the ionization volume are detected; all other trajectories are terminated by cryopumping on the shroud. The mass spectrometer, and hence the TPD experiment, is therefore blind to all gas sources except the emitting area within its line of sight. In the present study, the LOSMS method ensures that species generated by the impact of hot gaseous species on the internal surfaces of the vacuum chamber are not measured in the mass spectrum and do not affect the TPD experiment.

Ab Initio Calculations. Standard ab initio molecular orbital calculations were performed using the Gaussian 03 Rev.04 program package.[14] Conformation analysis of the IL was performed using B3LYP/6−31+G(d,p)[15] with help of the procedure developed in our previous work.[5]

Optimized structure, and energy of the most stable conformer of the ionic pair was further obtained using the G3MP2 and CBS-QB3 composite methods. The G3 theory is a procedure for calculating energies of molecules containing atoms of the first and second row of the periodic table based on ab initio molecular orbital theory. A modification of G3 theory that uses reduced orders of Møller−Plesset perturbation theory is the G3MP2 theory.[16,17] This method saves considerable computational time compared to the G3 theory with limited loss in accuracy but is much more accurate than G2(MP2) theory. G3(MP2) theory uses geometries from second-order perturbation theory and scaled zero-point energies from Hartree−Fock theory followed by a series of single-point energy calculations at the MP2(Full)/6−31G(d), QCISD(T)/6−31G(d), and MP2/GTMP2 Large levels of theory (for details, see ref 16). CBS-QB3 theory uses geometries from B3LYP/6−311G(2d,d,p) calculation and scaled zero-point energies from B3LYP/6−311G(2d,d,p) calculation followed by a series of single-point energy calculations at the MP2/6−311G(3df,2df,2p), MP4(SDQ)/6−31G(d(f),p), and CCSD(T)/6−31G levels of theory.[18] Calculated values of the enthalpy and Gibbs energy of ions and ion pairs are based on the electronic energy

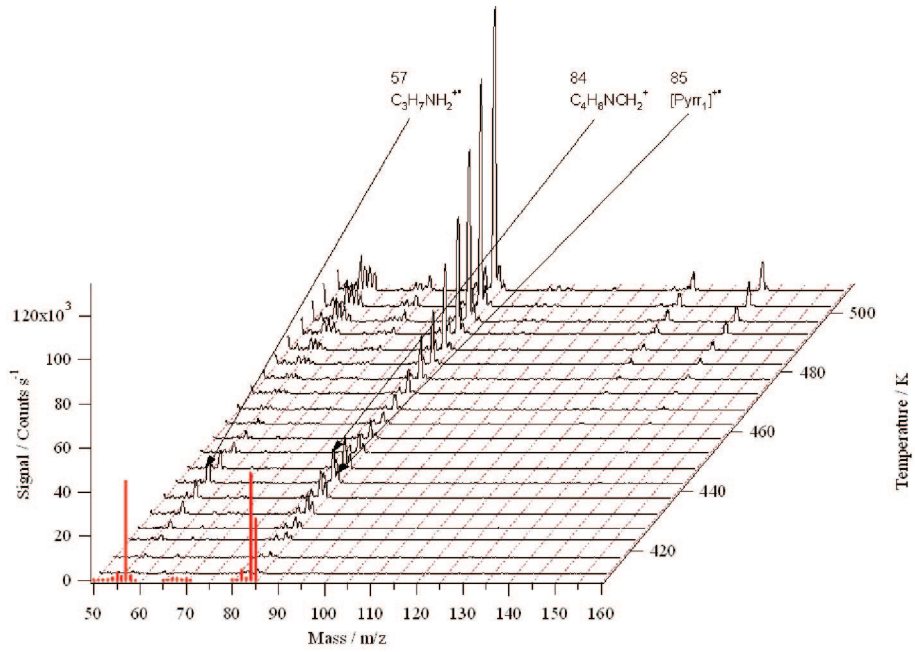

Figure 3. An expanded multiple mass spectra of $[Pyrr_{14}][dca]$ taken during temperature-programmed desorption showing contaminant peaks at lower temperatures. Masses 57, 84, and 85 are characteristic of 1-methylpyrrolidine, the cracking pattern of which is shown as a bar graph, taken from ref 23.

calculations obtained by the CBS-QB3 and G3MP2 methods using standard procedures of statistical thermodynamics.[19]

Results and Discussion

Combustion Calorimetry. Results of combustion experiments on $[Pyrr_{14}][dca]$ are summarized in the Tables 1−3. The value of the standard specific energy of combustion $\Delta_c u^\circ = -(34745.9 \pm 4.0)\ J\cdot g^{-1}$ has been used to derive the standard molar enthalpy of combustion $\Delta_c H^\circ_m = -(7244.8 \pm 2.3)\ kJ\cdot mol^{-1}$ and the standard molar enthalpy of formation in the liquid state $\Delta_f H^\circ_m(l) = (57.9 \pm 2.8)\ kJ\cdot mol^{-1}$ based on the reaction:

$$C_{11}H_{20}N_4 + 16\times O_2 = 11\times CO_2 + 10\times H_2O + 2\times N_2 \quad (2)$$

$\Delta_f H^\circ_m(l)$ of the $[Pyrr_{14}][dca]$ has been obtained from the enthalpic balance according to eq 3:

$$\Delta_f H^\circ_m(l,[Pyrr_{14}][dca]) = 11\times\Delta_f H^\circ_m(g, CO_2) + 10\times\Delta_f H^\circ_m(1, H_2O) - \Delta_c H^\circ_m \quad (3)$$

where molar enthalpies of formation of H_2O (l) and CO_2 (g) were taken from the literature, as assigned by CODATA.[8]

Molar Enthalpy of Vaporization $\Delta^g_l H_m$ of $[Pyrr_{14}][dca]$. Figure 2 shows multiple mass spectra taken during a TPD scan, as a plot of intensity versus temperature and mass. Clearly there is a desorption peak starting at ~500 K, which occurs for several masses. Figure 3 shows a detail of the low temperature part of this plot, where another desorption peak can be seen at about 440 K for masses in the $m/z = 58$ and 84 region; this is due to a contaminant desorption peak and is discussed below.

To show the mass spectrum of $[Pyrr_{14}][dca]$ more clearly, Figure 4a shows a high signal-to-noise mass spectrum obtained during isothermal desorption at 550 K, while Figure 4b shows a "true" but lower signal-to-noise spectrum which only contains peaks due to gases originating from the ionic liquid itself. (Figure 4b was obtained by measuring a mass spectrum over a 30 s period, flag out, then blocking the LOS beam with the flag, flag in, and measuring a second spectrum which only contained peaks due to emission within the mass spectrometer itself; by subtracting the second scan from the first, the spectrum due to the vapors originating directy from the IL is obtained). Figure 4b, true signal, exhibits peaks corresponding to m/z values of 142, 127, 86, 85, 84, 58, and 55 which are due to the IL vapor and any decompositon products produced at the sample. The peaks at 100, 98, and 70 (Figure 4a) are cracking products produced within the ionization region of mass spectrometer.

The peak at $m/z = 142$ is the cation of the ionic liquid, I, $[Pyrr_{14}]^+$ (see Figure 5). The peak at $m/z = 127$ corresponds to ion II, $C_4H_8N(C_4H_9)^{+\bullet}$, $[Pyrr_4]^{+\bullet}$, where a $CH_3\bullet$ has been lost from the parent cation, while the peak with the highest intensity, at $m/z = 84$ is IIIA, $C_4H_8NCH_2^+$, which is II after loss of $C_3H_7\bullet$. IIIA can be written as a series of resonance forms, which may explain its stability and hence greater intensity. There are also two smaller peaks at 85 and 86 which can be identified as IIIB, $[Pyrr_1]^{+\bullet}$ and IIIC, $[Pyrr_{1H}]^+$. The cracking pattern of $[Pyrr_{14}]^+$ will be discussed in greater detail in a forthcoming paper.[20] Values 58 and 55 could be IV, $C_3H_6NH_2^+$, and V, $C_4H_7^+$, respectively. The small peaks at 70, 98, and 100 are $C_4H_8N^+$ (VI), $C_4H_8N(C_2H_4)^+$ (VII), and $C_4H_8N(H)(C_2H_5)^+$ (VIII), respectively.

A search was made for the ionized ion pair species $\{[Pyrr_{14}][dca]\}^{+\bullet}$ at $m/z = 208$, and for the clusters $\{[Pyrr_{14}]_2[dca]\}^+$ (350) and $\{[Pyrr_{14}]_2[dca]_2\}^+$ (416), but all were undetected, placing their intensities below our detection limit of 10^{-5} of the $[Pyrr_{14}]^+$ ion intensity. From previous TPD studies of ILs,[10] it is expected that the $[Pyrr_{14}]^+[dca]^-$ will desorb as an ion pair (we have appended charges to the formulas to aid understanding of the following description). When the ion pair is ionized in the mass spectrometer, the transient species $\{[Pyrr_{14}]^+[dca]^-\}^{+\bullet}$ is produced. The $[Pyrr_{14}]^+$ cation in this species remains positively charged, but the electron ejected from the ion pair during ionization effectively comes from the anion, leaving it as the uncharged radical, [dca]•. The Coulombic bond holding the anion and cation together is therefore removed and

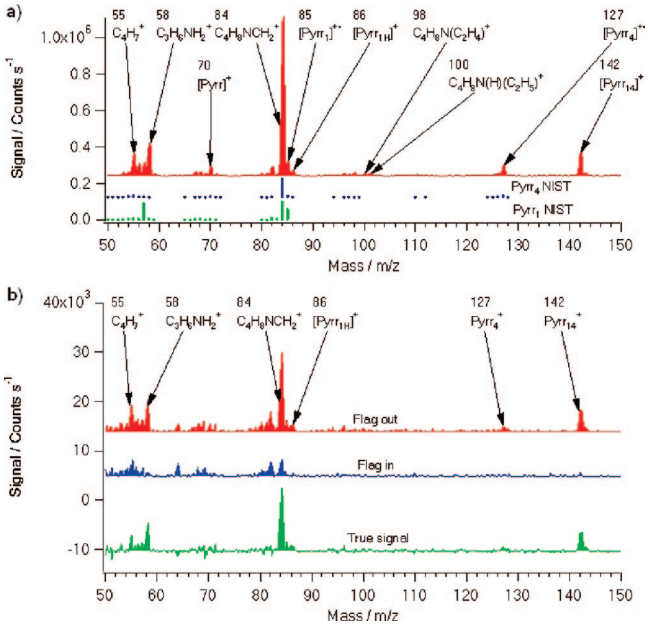

Figure 4. (a) Mass spectrum taken during isothermal desorption. At the bottom are shown the 1-methylpyrrolidine spectrum and 1-butylpyrrolidine spectrum (taken from the NIST database[23]). (b) Low signal-to-noise spectra used to identify species within the LOS beam. Flag in and flag out refer to the LOS beam being obscured and unobscured, respectively, while true signal is flag out − flag in.

the $[Pyrr_{14}]^+$ and [dca]• dissociate, presumably because of thermal excitation during the ionization process. Therefore, in the mass spectrum we see the $[Pyrr_{14}]^+$ ion but not the $\{[Pyrr^{14}]^+[dca]^-\}^{+\bullet}$ nor the [dca]• radical (as it is uncharged). The process can be written as follows:

$$[Pyrr_{14}]^+[dca]^- + e^- \rightarrow \{[Pyrr_{14}]^+[dca]^-\}^{+\bullet} + 2e^-$$

$$\{[Pyrr_{14}]^+[dca]^-\}^{+\bullet} \rightarrow [Pyrr_{14}]^+ + [dca]\bullet$$

$$[Pyrr_{14}]^+ \rightarrow \text{fragmentation products (II to V)}$$

If clusters such as $[Pyrr_{14}]_n[dca]_n$ were in the vapor, then one would not expect to see ions of the type $([Pyrr_{14}]_n[dca]_n)^{+\bullet}$ in the mass spectrum, but one would expect to see ions of the general formula $\{[Pyrr_{14}]_n[dca]_{n-1}\}^+$, for the same reasons as outlined above. Also, one might expect any $\{[Pyrr_{14}]_n[dca]_{n-1}\}^+$ ions to fragment to produce $\{[Pyrr_{14}]_2[dca]\}^+$ ions. As no $\{[Pyrr_{14}]_2[dca]\}^+$ ions were observed, it is strong evidence that there were no clusters in the vapor apart from ion pairs. In summary, the IL vapor consisted solely of ion pairs.

In the first TPD study of eight imidazolium cation, $[C_nC_mIm]^+$ based ILs[10] it was found that the highest *m/z* value in the mass spectrum was always due to the imidazolium cation itself ($[C_nC_mIm]$ corresponds to an imidazolium cation with alkyl chains containing *n* and *m* carbon atoms in the 1 and 3 positions). No clusters of any type were detected, and the ion signals disappeared on reducing the ionization energy to zero, showing that emission of positively charged particles from the IL did not occur. So both the imidazolium-based ILs and the pyrrolidinium-based IL reported here behave in the same manner, which can be summarized as:

(i) thermal evaporation of the IL occurs as neutral ion pairs;

(ii) ionization of neutral ion pairs within the mass spectrometer occurs by loss of an electron from the anion, turning it into an uncharged, neutral species;

(iii) the cation-neutral species combination dissociates such that only the cation and smaller *m/z* values are detected in the mass spectrometer.

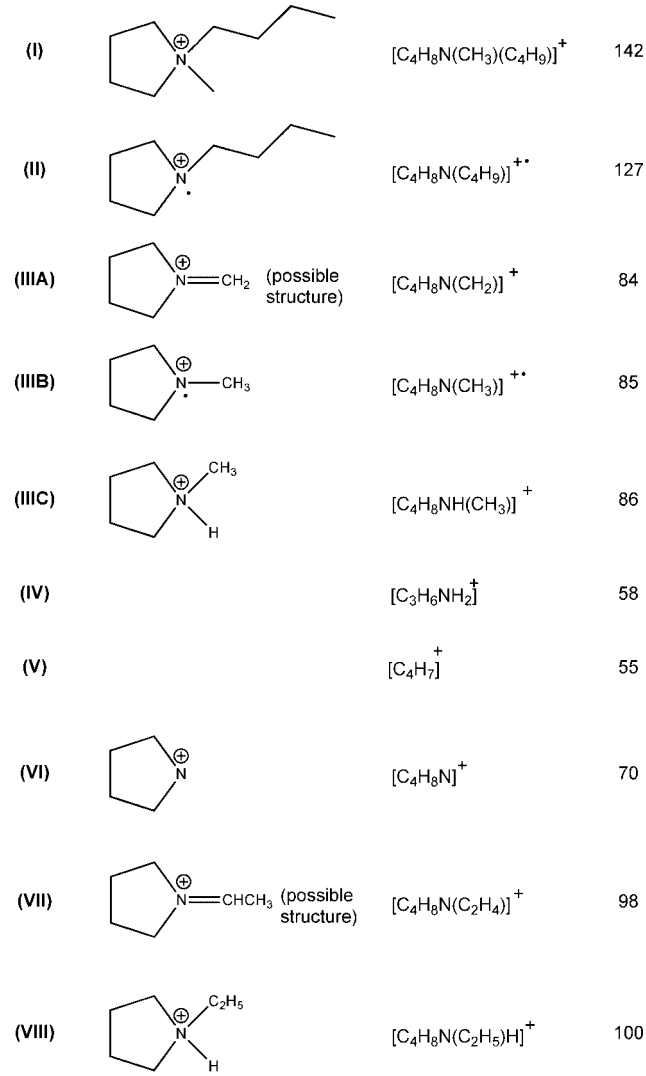

Figure 5. Formulas and possible structures for ions I−VIII.

Further publications are in preparation regarding reactions and fragmentations in steps ii and iii for imidazolium-, pyrrollidinium-, pyridinium-, and dication-based ILs with a range of anions.

The activation energy, E_a, and hence enthalpy, of vaporization were determined using TPD. From the above description of the cracking pattern of the IL, it can be seen that the intensity (*S*) of the $[Pyrr_{14}]^+$ ion (and its fragmentation products) will be proportional to the number density of the ion pair in the IL vapor. Figure 6 shows the intensity of the $[Pyrr_{14}]^+$ cation versus *T* for a heating rate of 0.052 K/s. For multilayer desorption, i.e. desorption from a thin film, we expect zero order kinetics[10] because the desorbing surface has a constant area. However, complications can arise if the evaporating surface area changes during the experiment due to the IL drying out on parts of the dip-stick and hence reducing the desorbing area. For this reason we only analyze the initial parts of the exponentially increasing rate of desorption, where we are confident that the surface area remains constant because no part of the film has dried out at that stage (Figure 6). By plotting ln(*S*) versus 1/*T*, a straight line is obtained (Figure 6) with a gradient $-E_a/R$. Five experiments were carried out at an average temperature of 500 K for the desorption analysis, giving $E_a(500\ K) = 137 \pm 2$ kJ mol^{-1} and hence $\Delta_f^g H_m$ (500 K) = 141 kJ mol^{-1}.

The experimental value of $\Delta_f^g H_m$ (500 K) was adjusted to the reference temperature of 298.15 K as described in refs 10

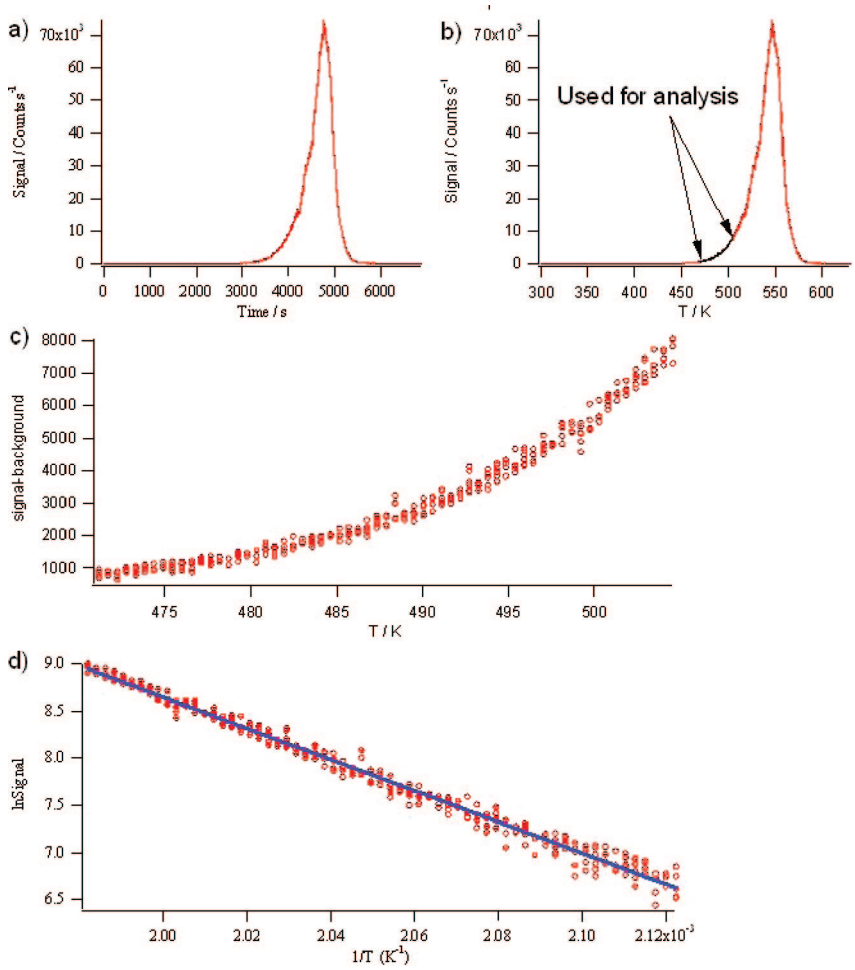

Figure 6. Example of TPD analysis using $m/z = 142$. (a) Full TPD curve (signal versus time). (b) Full TPD curve (signal versus temperature) with the part of curve used for analysis indicated. (c) The part of the TPD curve used to calculate E_a. (d) Plot of ln(signal) versus $1/T$, from which E_a was calculated.

and 21. The values of $\Delta_f^g C_p$ for [BMIM][dca] (−105.4 $J \cdot K^{-1} \cdot mol^{-1}$) and [BMIM][$PF_6$] (− 105.0 $J \cdot K^{-1} \cdot mol^{-1}$) are known from calorimetric data and statistical thermodynamic calculations.[5,22] Thus, the value $\Delta_f^g C_p = (-105.4\ J \cdot K^{-1} \cdot mol^{-1})$ could be also applied for [$Pyrr_{14}$][dca]. However, in order to remain consistent with our previous work,[10] in this paper the value of $\Delta_f^g C_p$used was − 94.0 $J \cdot K^{-1} \cdot mol^{-1}$. Using this value of $\Delta_f^g C_p$, $\Delta_f^g H_m$ (298.15 K) = 161.0 ± 2.0 kJ mol^{-1} (by using the value of $\Delta_f^g C_p = -105.4\ J \cdot K^{-1} \cdot mol^{-1}$, the vaporization enthalpy adjusted to the reference temperature will be $\Delta_f^g H_m$ (298.15 K) = 162.2 ± 2.0 kJ mol^{-1} and this value hardly differs within the boundaries of experimental uncertainties).

As mentioned above and shown in Figure 3, there was a peak in the TPD at about 440 K due to contamination, which occurred with major peaks at $m/z = 57$, 84, and 85. Within experimental error, the relative intensities of these peaks[23] are the same as for $Pyrr_1$, 1-methylpyrrolidine, see Figure 3, allowing us to identify the impurity as this compound. The lack of any peaks above $m/z = 85$ (within our limits of detection) rules out $Pyrr_4$, 1-butylpyrrolidine, as a possible contaminant. Without calibration, it is not possible to be quantitative as to the concentration of the impurity, but from the intensities of the IL and contaminant peaks in Figure 2, one would estimate that the contamination is <1%. An additional check of purity by NMR did not reveal this impurity, so we are confident that the real concentration was indeed low.

We now comment on the thermal stability of [$Pyrr_{14}$][dca]. According to studies using thermogravimetry (TGA), [$Pyrr_{14}$][dca] starts to decompose at 535 K.[24] This is because of the rather nucleophilic nature of the [dca] or $[N(CN)_2]^-$ anion. By contrast, the analogous ionic liquid, composed of the common cation and $[NTf_2]^-$ as the anion, decomposes at 672 K.[24] Figure 7 shows TPD curves for [$Pyrr_{14}$][dca] obtained using several different masses in a single TPD experimental run. The $[Pyrr_{14}]^+$ cation at $m/z = 142$ shows a smooth desorption profile, but lower masses show multiple sharp spikes in their signals which lie on top of an underlying smooth curve. Careful analysis shows that these spikes are due to pressure bursts in the vacuum chamber and can be seen for masses which were scanned sequentially, the signals decaying back to the underlying, smooth value over a period of about 10 s. The pressure spikes are caused by bubbles of decomposition products bursting at the surface of the thin IL film during TPD. The complete absence of spikes on the 142 mass signal shows that this mass monitors just the evaporation of the IL and hence the above analysis of the heat of vaporization is valid. Masses 57, 58, 84, 85, 86, and 127 have been shown (above) to be cracking fragments of $[Pyrr_{14}]^+$, and they are seen to have the same general underlying shape as the $m/z = 142$ peak. However, subtle differences can also be observed in these spectra. $m/z = 86$ shows very few pressure spikes and is very nearly the same shape as that for the $m/z = 142$ peak; this is consistent with this peak being almost exclusively formed by cracking of the parent cation. Values $m/z = 57$ and 85 show a clear desorption peak at about 450 K due to desorption of the $Pyrr_1$ contaminant; this peak exhibits no spikes, as it is not a decomposition product. The underlying

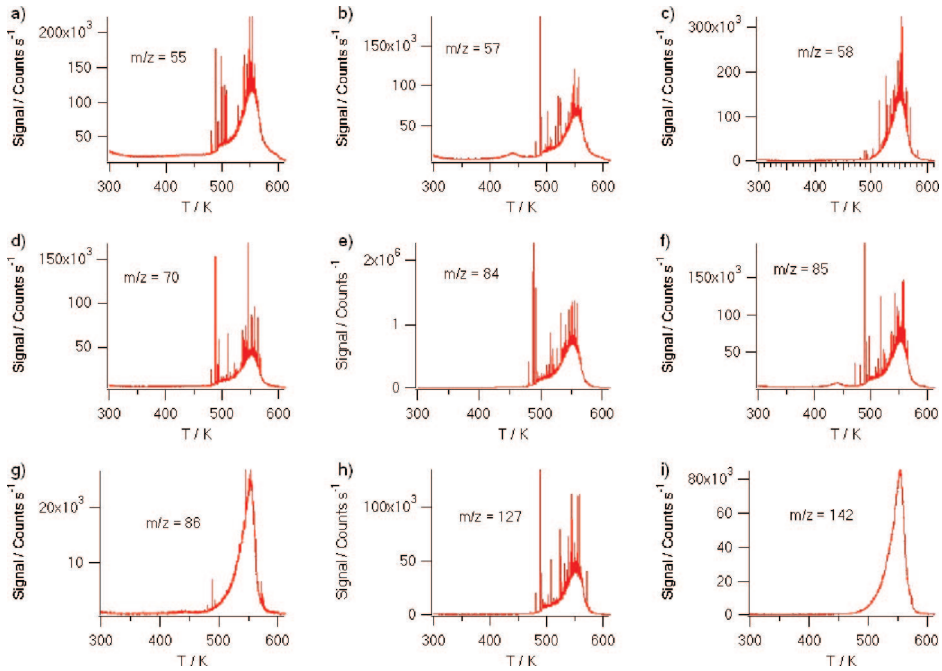

Figure 7. TPD curves of signal versus temperature for particular *m*/*z* values: (a) 55, (b) 57, (c) 58, (d) 70, (e) 84, (f) 85, (g) 86, (h) 127, (i) 142. The spikes are pressure jumps due to bubbles of decomposition products bursting at the surface of the thin IL film.

TABLE 4: G3MP2 and CBS-QB3 Enthalpies at 298.15 K (in Hartree)

	H_{298}		
compound	G3MP2	CBS-QB3	$\Delta_f H^\circ_{mexp.gas}$
methane	−40.418284	−40.406185	−74.9 ± 0.4 (ref 28)
ethane	−79.646714	−79.626127	−83.8 ± 0.3 (ref 28)
ammonium	−56.503209	−56.456375	−45.94 (ref 28)
pyrrolidine	−212.184151	−212.145856	−3.40 (ref 28)
[$Pyrr_{14}$][dca]	−649.035061	−648.929807	—

TABLE 5: Comparison of the Enthalpies of Formation $\Delta_f H^\circ_m$(gas) of [$Pyrr_{14}$][dca] Derived Using ab Initio Methods (in kJ·mol^{-1})

G3MP2			CBS-QB3		
AT	BS1	BS2	AT	BS1	BS2
222.3	217.2	213.4	229.2	210.1	211.7
	average 217.6			average 217.0	

curve for *m*/*z* = 55, although it has a shape similar to that of *m*/*z* = 142, is more rounded and has distinct shoulders at ~500 K and ~590 K. All the masses except *m*/*z* = 86 show a more rounded shape, with some also exhibiting the shoulder at 500 K. These observations can be accounted for if the IL is evaporating, decomposing smoothly, and decomposing by bubble formation as shown by the following scheme:

[$Pyrr_{14}$][dca] (l) → [$Pyrr_{14}$][dca] (g) smooth TPD curves at mass 142 and masses ≤ 127

[$Pyrr_{14}$][dca] (l) → decomposition products (g) smooth TPD curves at masses ≤ 127 except 86

[$Pyrr_{14}$][dca] (l) → decomposition products (gas bubbles) pressure spikes at masses ≤ 127 except 86

It should be noted that not all the desorption runs produced bubbles. We can only differentiate between species in the LOS beam (IL ion pairs and decomposition products from the IL on the dip-stick) and those generated within the mass spectrometer itself (due to vapor which has been deposited on hot surfaces within the mass spectrometer and subsequently desorbed and/or cracked). Therefore the TPD data for *m*/*z* ≤ 127 contain contributions from both the evaporating ionic liquid and decomposition products.

Kroon et al.[25] have investigated the thermal decomposition of ILs using ab initio quantum chemical calculations. On applying the ideas from their work to the decomposition of [$Pyrr_{14}$][dca] one would expect the following S_N2 reaction to occur, producing $Pyrr_4$, 1-butylpyrollidine, and the methylated dicyanamide

$$[Pyrr_{14}][dca] \rightarrow Pyrr_4 + H_3C - NCNCN$$

From Figure 7 it can be seen that pressure spikes occur for all the fragments of $Pyrr_4$ (see Figure 4a), with those for *m*/*z* = 84 being of much higher intensity than the other fragments. This is consistent with the pressure spikes, and hence the decomposition product, being due to $Pyrr_4$. However, we have not attempted to carry out a more precise analysis of the cracking pattern of the decomposition products from Figures 2 and 7. Clearly the smooth parts of the curves in Figure 7 are dominated by the zero order shape, but there is insufficient information to allow separation of the IL vapor and contaminant parts from these curves. Regarding the pressure spikes, they decayed too quickly to allow accurate comparisons of the mass intensities. Also, at the end of a TPD experiment an involatile carbonaceous film was left on the silver dipstick, showing that not all the decomposition products were volatile.

TABLE 6: Ab Initio G3MP2 Study of the Reaction of the Possible Decomposition of the [Pyrr$_{14}$][dca] at 298 K

[Pyrr$_{14}$][dca] = [Pyrr$_{14}$]$^+$ + [dca]$^-$			
$\Delta_r G°$, kJ·mol^{-1}	$\Delta_r H°$, kJ·mol^{-1}	$\Delta_r S°$, J·K^{-1}·mol^{-1}	K_p, Pa
307.9	346.8	130.5	1.1×10^{-54}

Ab Initio Results and Thermodynamics in the Gaseous Phase. The composite ab initio methods G3 and CBS have been used for calculations of the free cation [Pyrr$_{14}$]$^+$, the free anion [dca]$^-$, and the ion pair [Pyrr$_{14}$]$^+$ [dca]$^-$. The optimized structure of the ion pair is shown in Figure 1. On the basis of these quantum mechanical results, the Gibbs energy, the enthalpy, and the entropy at 298.15 K have been calculated using standard procedures of statistical thermodynamics.[19] The purpose of this procedure was to obtain absolute values of the standard Gibbs energy of reaction of dissociation of the ion pair [Pyrr$_{14}$]$^+$ [dca]$^-$ in the gaseous phase according to

$$[\mathrm{Pyrr}_{14}][\mathrm{dca}] = [\mathrm{Pyrr}_{14}]^+ + [\mathrm{dca}]^- \quad (4)$$

The results obtained are listed in Table 4. From the calculated theoretical results the chemical equilibrium constant K_p in the ideal gaseous state has been calculated according to

$$K_p = \exp[-\Delta_r G^o/RT] \quad (5)$$

from which the degree of dissociation of the ion pair α defined as

$$\alpha = \frac{p^+}{p_{IP} + p^+} = \frac{p^-}{p_{IP} + p^-} \quad (6)$$

can be calculated according to

$$K_p = \frac{\alpha^2}{1-\alpha^2} \times p_{sat} \quad (7)$$

or

$$\alpha = \sqrt{\frac{K_p/p_{sat}}{1 + K_p/p_{sat}}} \quad (8)$$

where $p^+ = p^-$ is the partial pressure of the cation and anion respectively, p_{IP} is the partial pressure of the ion pair and p_{sat} is the saturation pressure of the liquid related to these partial pressures by

$$p_{sat} = p_{IP} + p^+ + p^- \quad (9)$$

The results presented in Table 6 show that $K_p = 1.1 \times 10^{-54}$ is negligibly small; thus, it can be concluded with high reliability that α is zero, i.e. the ionic liquid [Pyrr$_{14}$][dca] exists exclusively as an ion pair in the gaseous phase in agreement with the experimental results.

Determination of the Gaseous Enthalpies of Formation of [Pyrr$_{14}$][dca]. The enthalpy of formation, $\Delta_f H°_m(l) = (57.9 \pm 2.8)$ kJ·mol^{-1}, of [Pyrr$_{14}$][dca], derived from the combustion experiments together with the vaporization enthalpy $\Delta^g_f Hm = (161.0 \pm 2.0)$ kJ·mol^{-1}, derived from the mass-spectroscopic measurements are referred to the reference temperature $T =$ 298.15 K. Using the equation $\Delta_f H°_m(g) = \Delta_f H°_m(l) + \Delta^g_f H_m$ we calculated value of the standard molar enthalpy of formation $\Delta_f H°_m(g) = (218.9 \pm 3.4)$ kJ·mol^{-1} which is to our knowledge the first experimental determination of this key thermodynamic property for the common pyrrolidinium-based (or quarternary ammonium-based) ionic liquids in the literature. This value has been used to check validity of ab initio methods as follows.

Quantum Chemical Calculations for $\Delta_f H°_m(g)$ of [Pyrr$_{14}$][dca]. Results of the molar enthalpy of formation, $\Delta_f H°_m(g)$, of ionic liquids obtained by using ab initio methods have not been reported in the literature so far. In standard Gaussian-n theories, theoretical enthalpies of formation in the gaseous state are calculated using atomization reactions.[26] Raghavachari et al.[27] have proposed to use a set of isodesmic reactions, the "bond separation reactions", to derive theoretical enthalpies of formation. Isodesmic reactions conserve the number of types of bonds and therefore should provide an improvement compared to simple atomization reactions. Further enhancement in the calculation of enthalpies of formation should be provided by isodesmic reactions, which, in addition to the types of bonds also conserve the hybridization of the atoms in the bond. We have calculated the enthalpies of formation of [Pyrr$_{14}$][dca] using G3MP2 and CBS-QB3 methods applying both standard atomization reactions and isodesmic reactions. For the latter method we have chosen the following two reactions:

$$[\mathrm{Pyrr}_{14}][\mathrm{dca}] + 25\ \mathrm{CH_4} = 4\ \mathrm{NH_3} + 18\ \mathrm{C_2H_6} \quad (10)$$

$$[\mathrm{Pyrr}_{14}][\mathrm{dca}] + 19\ \mathrm{CH_4} = 3\ \mathrm{NH_3} + \text{pyrrolidine} + 13\ \mathrm{C_2H_6} \quad (11)$$

Using enthalpies of these reactions calculated by G3MP2 and CBS-QB3 and enthalpies of formation $\Delta_f H°_m(g)$, for species involved in the reactions 10 and 11 recommended by Pedley et al.[28] the enthalpy of formation of [Pyrr$_{14}$][dca] has been calculated (see Tables 2 and 3). As presented in Table 3 the average value for $\Delta_f H°_m(g)$ calculated by G3MP2 and CBS-QB3 is in excellent agreement with the experimental value derived in this work. $\Delta_f H°_m(g)$ of [Pyrr$_{14}$][dca] derived by compound methods with help of the atomization procedure is also in excellent agreement with the experimental results.

Conclusions

The present study was undertaken to obtain the first experimental determination of the gaseous enthalpy of formation, $\Delta_f H°_m(g)$, of [Pyrr$_{14}$][dca], the enthalpy of vaporization for this ionic liquid, and the mass spectrum of its vapor. Such data would provide the indispensable basis for testing ab initio procedures and the quality of theoretically obtained prediction of the vapor pressure of RTILs using MD-simulation technique supported by quantum-mechanical ab initio calculations.

Acknowledgment. This work has been supported by German Science Foundation (DFG) SPP1191. V.E. gratefully acknowledges a research scholarship from the Research Training Group "New Methods for Sustainability in Catalysis and Technique" of the German Science Foundation (DFG). We thank the University of Nottingham and the EPSRC for financial support. P.L. acknowledges EPSRC for the award of an ARF (EP/D073014/1).

References and Notes

(1) Wasserscheid, P.; Welton, T. *Ionic liquids in synthesis*; Wiley-VCH: New York, 2002.

(2) MacFarlane, D. R.; Golding, J.; Fortsyth, S.; Fortsyth, M.; Deacon, G. *Chem. Commun.* **2001**, 1430–1431.

(3) MacFarlane, D. R.; Golding, J. *Chem. Commun.* **2001**, *16*, 1430–1431.

(4) Verevkin, S. P.; Beckhaus, H. D.; Rüchardt, C.; Haag, R.; Kozhushkov, S. I.; Zyweitz, T.; de Meijere, A.; Jiao, H.; Schleyer, P. *J. Am. Chem. Soc.* **1998**, *120*, 11130.

(5) Emel'yanenko, V. N.; Verevkin, S. P.; Heintz, A. *J. Am. Chem. Soc.* **2007**, *129*, 3930.

(6) Atomic weights of the elements. Review 2000. *Pure Appl. Chem.* **2003**, *75*, 683.

(7) Hubbard, W. N.; Scott, D. W.; Waddington, G. *Experimental Thermochemistry*; Rossini, F. D., Ed.; Interscience: New York, 1956; p 75.

(8) *CODATA Key Values for Thermodynamics*; Cox, J. D.; Wagman, D. D.; Medvedev, V. A., Eds.; Hemisphere: New York, 1989.

(9) Olofsson G. *Combustion calorimetry*; Sunner, S.; Mansson, M., Eds.; Pergamon: New York, 1979; Chapt. 6.

(10) Armstrong, J. P.; Hurst, C.; Jones, R. G.; Licence, P.; Lovelock, K. R.; Satterley, C. J.; Villar-Garcia, I. J. *Phys. Chem. Chem. Phys.* **2007**, *9*, 982–990.

(11) Jones, R. G.; Fisher, C. J. *Surf. Sci.* **1999**, *24*, 127.

(12) Jones, R. G.; Clifford, C. A. *Phys. Chem. Chem. Phys.* **1999**, *1*, 5223.

(13) Chan, A. S. Y.; Skegg, M. P.; Jones, R. G. *J. Vac. Sci. Technol. A* **2001**, *19*, 2007.

(14) Frisch, M. J. et al. Gaussian 03, Revision B.04; Gaussian, Inc.: Pittsburgh PA, 2003.

(15) Hill, R. A.; Labanowski, J. K.; Heisterberg, J. D.; Miller, D. D. In *Density functional methods in chemistry*; Labanowski, J. K., Andyelm, J. W., Eds.;Springer-Verlag: New York, 1986.

(16) Curtiss, L. A.; Redfern, P. C.; Raghavachari, K.; Rassolov, V.; Pople, J. A. *J. Chem. Phys.* **1999**, *110*, 4703.

(17) Curtiss, L. A.; Redfern, P. C.; Raghavachari, K.; Rassolov, V.; Pople, J. A. *J. Chem. Phys.* **1998**, *109*, 7764.

(18) Montgomery, J. A.; Frisch, M. J., Jr.; Ochterski, J. W.; Petersson, G. A. *J. Chem. Phys.* **2000**, *112*, 6532–6542.

(19) McQuarrie D. A. *Statistical Mechanics*; Harper & Row: New York, 1976.

(20) Lovelock, K. R. J.; Deyko, A.; Licence, P.; Jones, R. G. Manuscript in preparation.

(21) Chickos, J. S.; Acree, W. E., Jr. *J. Phys. Chem. Ref. Data* **2003**, *32*, 519.

(22) Zaitsau, D. H.; Kabo, G. J.; Strechan, A. A.; Paulechka, Y. U.; Tschersich, A.; Verevkin, S. P.; Heintz, A. *J. Phys. Chem. A* **2006**, *110*, 7303.

(23) NIST Chemistry webbook. NIST Standard Reference Database Number 69, June 2005 Release. http://webbook.nist.gov/chemistry/.

(24) Wooster, T. J.; Johanson, K. M.; MacFarlane, D. R.; Scott, J. L. *Green Chem.* **2006**, *8*, 691–696.

(25) Kroon, M. C.; Buijs, W.; Peters, C. J.; Witkamp, G. J. *Thermochim. Acta* **2007**, *465*, 40.

(26) Notario, R.; Castaño, O.; Abboud, J.-L. M.; Gomperts, R.; Frutos, L. M.; Palmeiro, R. *J. Org. Chem.* **1999**, *64*, 9011.

(27) Raghavachari, K.; Stephanov, B. B.; Curtiss, L. *J. Chem. Phys.* **1997**, *106*, 6764.

(28) Pedley, J. P.; Naylor, R. D.; Kirby, S. P. *Thermochemical Data of OrganicCompounds*, 2nd ed.; Chapman and Hall: London, 1986.

JP803238T